

Extended Defect States in CdTe/ZnTe Photojunction

B.A. ORLOWSKI^{a,*}, K. GWOZDZ^b,
K. GOSCINSKI^a, S. CHUSNUTDINOW^a, M. GALICKA^a,
E. GUZIEWICZ^a AND B.J. KOWALSKI^a

^a*Institute of Physics, Polish Academy of Sciences, al. Lotnikow 32/46, Warsaw, PL-02668*

^b*Wroclaw University of Science and Technology,
Wybrzeze Wyspianskiego 27, 50-370 Wroclaw, Poland*

Received: 03.02.2022 & Accepted: 29.03.2022

Doi: [10.12693/APhysPolA.141.548](https://doi.org/10.12693/APhysPolA.141.548)

*e-mail: orbro@ifpan.edu.pl

The paper concerns the influence of defects states on the open-circuit voltage (V_{oc}) of a semiconductor photocell illuminated with different light intensity. The measured V_{oc} versus the number of photons (illumination intensity) curve is compared with the analogous dependence described by the theoretical model applied. Illumination of a semiconductor leads to a shift of the energy position of the quasi Fermi level relative to the Fermi level in thermal equilibrium. As the illumination intensity increases, the energy of the quasi Fermi level of electrons and holes shifts and influences directly the V_{oc} value. The defects existing inside the band gap contribute adequately to the structure of V_{oc} versus illumination intensity dependence due to the exchange interaction between free carriers and defect states, which appears in the case of energy coincidence. Comparison of V_{oc} measured and predicted by the proposed model for a specific illumination intensity allows the determination of the energy of defect states in the band gap. The extending defects damping of V_{oc} were studied for the p-ZnTe/n-CdTe photocell, and the results were compared with those obtained for the Si-based photocell. Value of open-circuit voltage was measured for a sample illuminated by a controlled number of laser photons that appear in bunches. The structure of V_{oc} versus illumination intensity curve for the ZnTe/CdTe photocell reveals four discrete defects states related to dislocations and located at the energies 26.6, 43.4, 57.0 and 67.4 meV below the Fermi level at thermal equilibrium.

topics: semiconductors photojunction, Fermi level shift, defect states, exchange interaction

1. Introduction

A photovoltaic heterojunction can be formed between two semiconductors [1–8], which have different crystalline and electronic structures and exhibit different types of conductivity (n and p on opposite sides). In spite of efforts to make such an interface as sharp and perfect as possible, it is difficult to avoid the formation of some lattice defects that relax strains between mismatched crystals, such as point defects (anti-sites, vacancies) or dislocations. The appearing lattice defects lead to the formation of electronic states, strongly modifying the parameters of the constructed heterojunction.

In this paper, we further explore the model proposed in [9]. It describes the photo-generation of an open-circuit voltage (V_{oc}) in a cell, based on a semiconductor heterojunction. The model uses the basic parameters describing the materials of the cell and enables us to estimate the values of V_{oc} expected for such a photocell illuminated by bunches

of monochromatic photons. In this paper, we consider the influence of defect-related electronic states on the measured V_{oc} . The discrepancy between the results of experiments and the calculated V_{oc} vs illumination dependence allows the derivation of the energy of defects modifying the properties of the heterostructure. These include extended defects related to dislocations, spontaneously formed quantum wells or quantum dots. Such a modification may be based on an exchange interaction between free electrons and electrons bound on dislocation states [6, 7] or other extended defects located in the junction region. Schröter [8] described these types of states as deep electronic states appearing at the extended defects. From these states, electrons could be exchanged with the conduction band in the processes of electron emission and capture. The relation between the rate of reaching internal equilibrium and the rates of capture and emission allowed these defect-related states to be classified as localized or band-like.

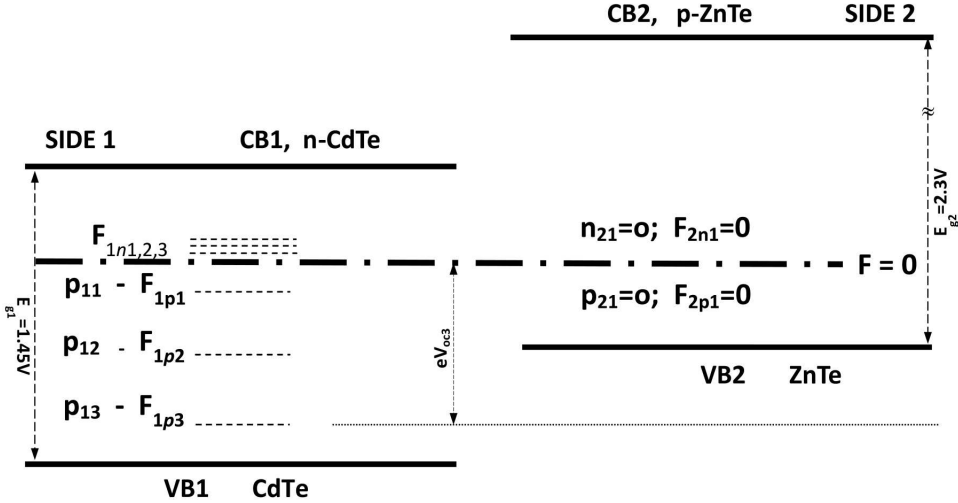


Fig. 1. The energy diagram of the n-CdTe/p-ZnTe photocell for moderate illumination intensity $F_{1p1} = k_B T \ln(p_{11}/p_{10}) \gg k_B T \ln(n_{11}/n_{10})$ [9]. The energy levels are shown relatively to the Fermi level in thermal equilibrium state. For the case of a moderate illumination, minority holes p_{11} , p_{12} or p_{13} and the corresponding energy shifts of quasi Fermi levels F_{1p1} , F_{1p2} or F_{1p3} contribute to the measured V_{oc} value. Here, V_{oc3} indicates a distance of the F_{1p3}/e level from the Fermi level position at thermal equilibrium. Three quasi Fermi level shifts of electrons ($F_{1n1,2,3}$) are negligibly small because of high concentration of majority carriers (electrons) in thermal equilibrium (e.g. $n_{10} = 10^{16} \text{cm}^{-3} \gg p_{10} = 10^6 \text{cm}^{-3}$).

The obtained results of experiments and model considerations can be correlated with the results of deep level transient spectroscopy (DLTS) studies [10, 11]. For the CdTe/ZnTe junction, the authors revealed, based on the DLTS temperature dependence spectra, the features attributed to extended and local defect states. Those states were related to a trap occurring in the CdTe layer or at the CdTe/ZnTe interface.

The first part of the paper presents the model [9] adapted to the case of the CdTe/ZnTe photojunction illuminated with photons absorbed only in the CdTe layer. The next part of the paper compares the related experimental results with the conclusions derived from the presented model.

2. The model

Let us consider the band structure of a junction of two different semiconductor crystals, i.e., n-type CdTe (see Fig. 1, side 1) and p-type ZnTe (side 2). Both sides have the thermal equilibrium Fermi level at the energy of $F = 0$. The position of the Fermi level within the energy gap on both sides of the junction describes the thermal equilibrium concentration of free electrons and holes, i.e., n_{10} and p_{10} as well as n_{20} and p_{20} , in the conduction and valence bands, respectively. Illumination of the sample increases the concentration of electrons and holes until a steady state is reached, with the corresponding carrier concentrations n_{11} , p_{11} and n_{21} , p_{21} in these two crystals. The achieved state can be described in terms of quasi Fermi levels and their shifts from the $F = 0$ energy. The quasi Fermi level

positions for the side 1 (CdTe) are given as $F_{1n1,2,3}$, F_{1p1} , F_{1p2} , F_{1p3} , provided all photons are absorbed in CdTe (Fig. 1).

The shifts of the quasi Fermi levels (e.g. $F_{1p1} = k_B T \ln(p_{11}/p_{10})$) correspond to changes in the chemical potential resulting from the generation of free carriers under the sample illumination [9]. These energy shifts contribute to the total V_{oc} value corresponding to the created steady state conditions. The contributions of electron and hole to V_{oc} equal $(F_{2n1} - F_{1n1})/e$ and $(F_{2p1} - F_{1p1})/e$, respectively, and so V_{oc} is determined by the following sum $(F_{2n1} - F_{1n1})/e + (F_{2p1} - F_{1p1})/e$. For a moderate value of carriers generation, the shifts of quasi Fermi levels of the majority carriers can be neglected, and thus V_{oc} can be described by the formula $(F_{1p1} + F_{2n1})/e$, where F_{1p1} and F_{2n1} are the quasi Fermi level shifts of the minority carriers on both sides of the junction. Moderate generation of minority carriers, e.g. $p_{11} = 100p_{10}$ in CdTe only (side 1) will be used to model the experimental results and to derive the relation $V_{oc} = F_{1p1}/e$ from open-circuit photovoltage as a function of the photon energy suitable for the carrier generation in n-type CdTe.

3. Experimental conditions

The investigated photocell consists of heterojunctions of p-ZnTe and n-CdTe. The structure was grown by molecular beam epitaxy (MBE) in an ultrahigh vacuum EPI 620 MBE system [12]. The highly I-doped n-CdTe buffer was grown on a GaAs(100) substrate. It was then covered with

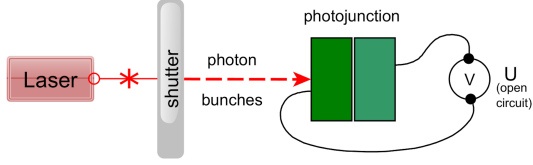


Fig. 2. The experimental setup used for V_{oc} versus light intensity measurements.

a layer of undoped CdTe and subsequently with N-doped p-ZnTe. Details of the heterostructure fabrication process can be found in [12]. In a general case of photojunction, the hole and electron densities in n-CdTe are $10^4 < p_{10} < 10^{10} \text{ cm}^{-3}$ and $10^{14} < n_{10} < 10^{17} \text{ cm}^{-3}$, respectively.

In the CdTe layers, a high density of dislocations ranging from 10^8 to 10^9 cm^{-2} was measured [13, 14]. It can be expected that during CdTe layers' growth in the photojunction technology procedure, this concentration value increases and a common electronic structure of defects can be formed, influencing its properties.

The sample is illuminated by a monochromatic laser beam chopped by a shutter into bunches of photons. The sample illumination intensity is governed by the shutter opening time (from 0.1667 up to 3.333 ms). The top layer of the photocell, made of ZnTe ($E_g^{\text{ZnTe}} = 2.25 \text{ eV}$), is transparent to photons with an energy of 1.91 eV applied in the experiment, while these photon bunches are absorbed in the CdTe layer ($h\nu > E_g^{\text{CdTe}} = 1.45 \text{ eV}$). As a result, the concentration of electrons and holes in the CdTe side of the photocell is assumed to be proportional to the number of photons in a single absorbed bunch, provided that a steady state is achieved in the heterostructure. The resulting photovoltage V_{oc} is measured in an open circuit configuration (Fig. 2).

4. Illumination conditions

If the number of photons in the bunch impinging the sample is B_i , the reflection, scattering on the sample surface and parasitic absorption reduce the number of photons to $B_g = rB_i$. These photons generate free holes and electrons in the active region of the photocell with the yield of g . So, the number of generated electron-hole pairs equals

$$B_f = B_g g. \quad (1)$$

The number of free electrons and holes generated in the heterojunction is reduced by the interaction with the environment in the crystal, e.g. by recombination, trapping, etc. The total yield of those processes is f_n for electrons and f_p for holes. As a result, a steady state is achieved in the illuminated system with the concentrations of free electrons and holes equal to n_{11} and p_{11} . These are given, respectively, as

$$n_{11} = B_f f_n, \quad (2)$$

and

$$p_{11} = B_f f_p, \quad (3)$$

and allow to determine the shifts of the corresponding quasi Fermi levels in the CdTe part of the cell (side 1). We assume that the coefficients r , g , f_p , f_n are constant for the constant photon energy and within the applied light intensity range. The analysis of the acquired experimental data will be based on the assumption that the number of generated carriers, in particular minority ones, is proportional to the number of photons in the bunch. This assumption would not be fulfilled if the photons scattered within the surface layer could efficiently generate additional electron-hole pairs. That may lead to the bowing of V_{oc} with respect to the number of photons (Fig. 3).

Increasing the number of photons in the bunches illuminating the sample, we will reach the threshold number of photons B_s at which V_{oc} starts to increase with the increase of illumination intensity. The increase in V_{oc} and the corresponding shift of the quasi Fermi level from 0 up to 60 meV requires a tenfold increase in illumination, as

$$F_{1p1} = k_B T \ln \left(\frac{p_{11}}{p_{10}} \right) = k_B T \ln \left(\frac{10B_s}{B_s} \right) =$$

$$\ln(10) \times 0.026 \text{ eV} \simeq 60 \text{ meV}. \quad (4)$$

Each further increase in the number of photons by an order of magnitude increases the V_{oc} value by another 60 meV (e.g. $10B_s \simeq 60 \text{ meV}$, $100B_s \simeq 120 \text{ meV}$, $1000B_s \simeq 180 \text{ meV}$).

Let us estimate the quasi Fermi level shifts of F_{1p1} and F_{1n1} for the n-CdTe sample (side 1), with the concentration of minority holes $p_{10} = 10^6 \text{ cm}^{-3}$ and the concentration of majority electrons $n_{10} = 10^{16} \text{ cm}^{-3}$ under moderate intensity of illumination. The illumination generates electron-hole pairs with the concentration of 10^8 cm^{-3} . Then $p_{11} = 100p_{10}$ and for minority carriers we obtain

$$F_{1p1} = k_B T \ln \left(\frac{p_{11}}{p_{10}} \right) =$$

$$\ln(100) \times 26 \text{ meV} \simeq 120 \text{ meV}, \quad (5)$$

while for majority carriers (electrons) $n_{10} = 10^{16} \text{ cm}^{-3}$ and $n_{11} = (10^{16} + 10^8) \text{ cm}^{-3}$, we have

$$F_{1n1} = \ln \left(\frac{10^{16} + 10^8}{10^{16}} \right) \times 26 \text{ meV} \simeq 0. \quad (6)$$

The value of F_{1n1} for majority carriers can be neglected compared to 120 meV for minority carriers. In this case, the quasi Fermi level holes F_{1p1} decide on the measured open-circuit voltage V_{oc} and its contribution to the V_{oc} illumination intensity dependence curve. The energy shift of the minority carriers of the quasi Fermi level, F_{1p1} , is the dominant contribution to the generated V_{oc} value and other parameters such as F_{1n1} , F_{2n1} , and F_{2p1} can be neglected.

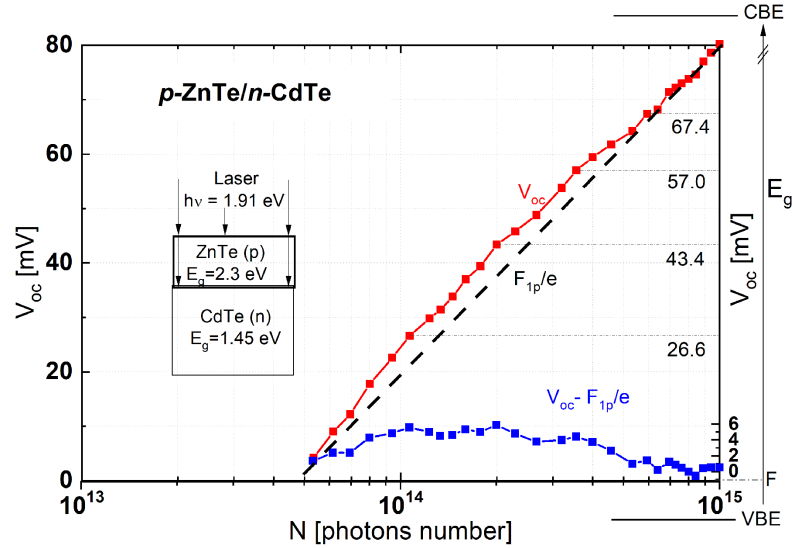


Fig. 3. The comparison of the experimental and theoretical V_{oc} versus illumination intensity curve for the p-ZnTe/n-CdTe of photocell [9]. The heterostructure is illuminated from the ZnTe side with photon bunches of energy $h\nu = 1.91$ eV coming from the laser. The ZnTe layer ($E_g = 2.3$ eV) is transparent to the light and absorbed by the CdTe ($E_g = 1.45$ eV) layer. The red curve presents measured experimental V_{oc} values for different illumination intensity. The black dashed line presents the V_{oc} values predicted by the model for different illumination intensity, while the blue curve presents the difference between the experimental and the model curves. The peaks visible in the lowest curve, as well as the steps on the experimental curve illustrate the effect of extending defect states influencing the V_{oc} value. The right hand side energy scale indicates the steps of the quasi Fermi level energy position corresponding to the measured V_{oc} values of 26.6, 43.4, 57.0, and 67.4 meV located below the thermal equilibrium Fermi level $F = 0$.

5. Experimental results

The measurements reported here were performed to study V_{oc} as a function of illumination intensity for side 1 of the photocell (n-CdTe/p-ZnTe) with a moderately small generation of electrons and holes. The energy of photons $h\nu = 1.9$ eV, located between the ZnTe and CdTe band gap (2.25 and 1.45 eV, respectively), ensured that the light was absorbed only in the n-CdTe layer. Low illumination intensity allows neglecting the contribution of quasi Fermi level shifts F_{1n1} related to the majority carriers to V_{oc} under steady state conditions.

The difference between the experimental curve with particular four steps (red curve in Fig. 3) and the linear dependence predicted by the model not taking into account any damping defects states (black dashed line in Fig. 3) resulted in the lowest difference curve, which consists of a set of peaks (blue curve in Fig. 3). The steps observed in the experimental curve and the related peaks visible in the difference curve can be understood in terms of the exchange interaction between free holes in the valence band with extended defect states. This kind of interaction occurs when the energy position of the quasi Fermi level approaches the energy position of the extended defect states. As a result, the appearance of four steps on the V_{oc} versus illumination dependence can be treated as caused by damping the concentration of free holes in the valence

band, caused by the exchange interaction with the extended defect states. The free holes will partially be trapped in extended defect states of dislocation and partially recombine with electrons.

The bowing of the experimental curve and the corresponding bowing of the difference curve presented at the bottom (blue line, Fig. 3) is caused by photons scattered on the surface, generating additional electrons and holes contributing to the measured V_{oc} (scattered photons contribution).

Concluding, one can say that scanning of the forbidden energy gap by the quasi Fermi level leads to the activation of particular defect centers, and that reduces the concentration of free holes (minority carriers) in the valence band, creates the steps observed in the experimental V_{oc} curve, and leads to further deviation of V_{oc} from the expected linear dependence, and finally decreases the generated minority carriers concentration through capture and recombination with electrons. In a further stage of illumination, the damping of the concentration of free holes caused by exchange interaction leads to the extended defects states saturation and finally reduces the damping effect to zero. For further measurements, the V_{oc} versus illumination intensity curve returns to the previous slope parallel to the slope predicted by the model. However, the value of V_{oc} shifts down to a value lower than that predicted by the model. The described creation of the V_{oc} step can be repeated for the next extended defect states

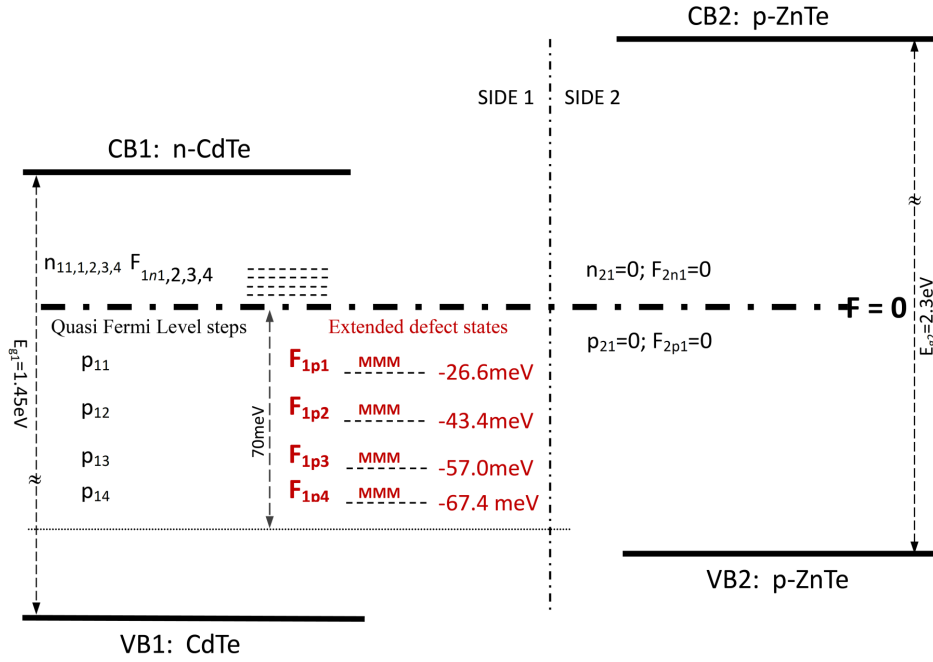


Fig. 4. The energy band diagram of the p-ZnTe/n-CdTe photocell showing the energy positions of extended defect states shown in Fig.3. Four extended defects energy levels are located at 26.6, 43.4, 57.0 and 67.4 meV below the Fermi level F and correlate with the set of values of holes and related quasi Fermi level energy.

when its energy is reached by the quasi Fermi level shifted after higher illumination. That will lead to the creation of the next step in the measured V_{oc} versus illumination intensity curve, which is reached for higher illumination. In this way, the set of extended defects states and dislocations can be occupied by minority carriers. This phenomenon leads to the creation of the obtained four sequential steps in the V_{oc} illumination intensity curve, which is caused by extended defect states related to dislocations. In this way, the measured set of four V_{oc} steps and the following step saturations can be linked with the energy positions of the extended damping defects states. The properties of defects strongly argue for treating them as a sequence of extended defects states related to dislocations, which are caused by the exchange interaction between free holes and the defect states.

The exchange interaction of free holes with extended defects states leads to the capture of the free carriers from the valence band, and it leads to a corresponding shift of the quasi Fermi level and the appearance of the step in V_{oc} versus illumination intensity curve. That increases the occupation of extended defect states and the probability of recombination of the carriers. The quasi Fermi level is pinned to the binding energy of the extended defects states, and the occupation of these states increases up to the saturation state. Summarizing the process, the free holes concentration is governed by an increase in recombination and the trapping of holes in the dislocation-related states until their occupation is saturated. For the saturated state, when

the trapping of holes stops, the slope of the V_{oc} illumination dependence returns to the previous value predicted by the model for the perfect heterojunction. The process repeats when the shifting, due to increasing illumination intensity, of the quasi Fermi level approaches the next level of the extended defect states. Then, the next step-like feature in the V_{oc} illumination intensity curve appears.

The presented model and the corresponding results of V_{oc} vs illumination intensity measurements show directly that the photovoltaic effect is strongly correlated to the change of the concentration of free minority carriers in the n-CdTe valence band. The relation V_{oc} vs illumination intensity curves allows to determine the sequence of energy positions of the four extended defects electronic levels located in the region close to the thermal equilibrium Fermi level (see Fig. 4). The presence of electronic states connected with extended defects in the ZnTe/CdTe junction was revealed by DLTS and reported in [10]. Three of them were ascribed to the majority hole traps occurring in CdTe. The DLTS characteristics of the fourth switched from those of a majority trap for negative filling pulses to that of a minority trap for positive filling pulses. Both the majority and minority trap levels were ascribed to the continuum defect states of band-like or localized character (in line with the classification proposed by Schröter [8]), occurring in the absorber layer and at the CdTe/ZnTe interface. The character of these two types of states was distinguished by variation of the DLTS line induced by changing the filling pulse width. In both cases, the amplitude of the

DLTS signal exhibited a linear dependence on the logarithm of the filling pulse width. However, the maximum of the DLTS feature shifted with the increase of the filling pulse width towards lower temperatures only for the band-like states. The minority and majority trap levels were located close to the midgap of CdTe and can be correlated with the region of sequence of the four states observed in V_{oc} illumination intensity dependence. In the case of a high density of defects, the interaction of dislocations of various types with other defects (e.g. point defects, quantum wells) can modify the sequence of binding energies of discrete extended defects of the dislocation origin.

6. Conclusions

The dependence of V_{oc} versus illumination intensity was measured for the p-ZnTe/n-CdTe photocell for moderate illumination conditions. The sample was illuminated by bunches of monochromatic laser light of energy 1.91 eV, which was absorbed only in the n-CdTe layer.

Under the conditions of low illumination intensity, the Fermi level shift of majority carriers (electrons) caused by the increased illumination can be neglected, so only a shift of minority carriers (holes) leads to the scanning of the valence band gap by the quasi Fermi level of n-CdTe. The exchange interaction between free carriers and carriers bound on dislocations is the origin of the observed deviation of the V_{oc} versus illumination intensity dependence from the theoretical linear dependence. The steps and saturation regions measured in the V_{oc} illumination intensity dependence allows determining the energies of four extended defects states, which can be treated as related to the dislocations origin 26.6, 43.4, 57.0 and 67.4 meV, located close to the Fermi level in thermal equilibrium.

The method used in the study might be promising to investigate the contribution of quantum structure effects (quantum defects, quantum wells, quantum dots) introduced to the interface region of a photojunction and influence its properties.

Acknowledgments

This work was partly supported by the Polish National Science Centre (NCN) Grant No. UMO-2016/21/B/ST5/03378.

References

- [1] S.M. Sze, *Semiconductor Devices: Physics and Technology*, Wiley, 2001.
- [2] J. Nelson, *The Physics of Solar Cells*, Imperial College Press, London 2003.
- [3] O. Yastrubchak, T. Wosinski, T. Figielski, E. Lusakowska, B. Pecz, A.L. Toth, *Physica E* **17**, 561 (2003).
- [4] L. Sosnowski, B. Orlowski, *Phys. Status Solidi A* **3**, 117 (1970).
- [5] A.A.M. Farag, I. S. Yahia, T. Wojtowicz, G. Karczewski, *J. Phys. D: Appl. Phys.* **43**, 215102 (2010).
- [6] T. Figielski, *Zjawiska Nierównowagowe w Półprzewodnikach*, Państwowe Wydawnictwa Naukowe, Warszawa 1980.
- [7] T. Figielski, *Solid State Electron.* **21**, 1403 (1978).
- [8] W. Schröter, J. Kronewitz, U. Gnauert, F. Riedel, M. Seibt, *Phys. Rev. B* **52**, 13726 (1995).
- [9] B.A. Orlowski, K. Gwozdz, M. Galicka, S. Chusnutdinow, E. Placzek-Popko, M.A. Pietrzyk, E. Guziejewicz, B.J. Kowalski, *Acta Phys. Pol. A* **134**, 590 (2018).
- [10] E. Zielony, K. Olender, E. Placzek-Popko, T. Wosiński, A. Racino, Z. Gumienny, G. Karczewski, S. Chusnutdinow, *J. Appl. Phys.* **115**, 244501 (2014).
- [11] K. Wichrowska, T. Wosinski, Z. Tkaczyk, V. Kolkovsky, G. Karczewski, *J. Appl. Phys.* **123**, 161522 (2018).
- [12] S. Chusnutdinow, R. Pietruszka, W. Zaleszczyk, V.P. Makhniy, M. Wiater, V. Kolkovsky, T. Wojtowicz, G. Karczewski, *Acta Phys. Pol. A* **126**, 1072 (2014).
- [13] J. Domagała, J. Bąk-Misiuk, J. Adamczewska, Z.R. Zytkeiwicz, E. Dynowska, J. Trela, D. Dobosz, E. Janik, M. Leszczyński, *Phys. Status Solidi A* **171**, 289 (1999).
- [14] A. Mycielski, A. Wardak, D. Kochanowska et al., *Prog. Cryst. Growth Charact. Mater.* **67**, 100543 (2021).